

Van Hove excitons and high- T_c superconductivity. I. Excitonic superconductivity

This article has been downloaded from IOPscience. Please scroll down to see the full text article.

1989 J. Phys.: Condens. Matter 1 8911

(<http://iopscience.iop.org/0953-8984/1/45/016>)

View [the table of contents for this issue](#), or go to the [journal homepage](#) for more

Download details:

IP Address: 171.66.16.96

The article was downloaded on 10/05/2010 at 20:57

Please note that [terms and conditions apply](#).

Van Hove excitons and high- T_c superconductivity: I. Excitonic superconductivity

R S Markiewicz†

Physics Department, Northeastern University, Boston, MA 02115, USA.

Received 10 October 1988, in final form 6 March 1989

Abstract. This paper presents a new variant of an excitonic model to explain the superconductivity in the high- T_c oxides. The carriers in the CuO_2 layers are divided into two groups: heavy and light holes. The heavy holes localise into a (charge) density wave, and it is virtual excitations across the density-wave gap which pair the light holes in a superconducting state. Such a mechanism can lead to strong deviations from BCS form for the temperature dependence of the gap. Comparison with experiment suggests that the density wave is present as two-dimensional fluctuations with long-range order setting in only near or below T_c . In $\text{La}_{2-x}\text{Sr}_x\text{CuO}_4$, it is suggested that materials with $x \neq 0$ or 0.15 are two-phase mixtures.

1. Introduction

Most properties suggest that the superconducting transition in the new high- T_c oxides [1, 2] is at least approximately governed by a BCS-like Hamiltonian. However, the question of what boson excitation causes the pairing remains unanswered. The very high values of T_c and the weakness of the isotope effect [3], especially in $\text{YBa}_2\text{Cu}_3\text{O}_{7-\delta}$ (YBCO) and related compounds, appear to rule out a pure phonon or bipolaron mechanism. Some sort of excitonic model has frequently been suggested as an alternative, and the observation of a low-energy optical feature in polycrystalline specimens, near 0.4 eV, has been taken as evidence for the required electronic excitation. Despite some initial evidence to the contrary [4], the preponderance of evidence from the last *APS March Meeting* suggests that this feature persists, albeit somewhat broadened, in single crystals and epitaxial films [5].

Even within an excitonic model, there are many different interpretations of the electronic transitions responsible for the 'exciton'. Little [6] has suggested that in YBCO the 'chain' electrons act as the excitons, but this cannot explain superconductivity in $\text{La}_{2-x}\text{Sr}_x\text{CuO}_4$ (LSCO) or the newer Bi- and Tl-based superconductors, which do not have chains. Varma *et al* [7] assume that the excitons are related to interband transitions between the Cu–O antibonding and non-bonding bands. In the present paper, yet another model of these excitons is proposed. These new excitons are closely associated with the van Hove singularity in these materials.

The van Hove singularity in question occurs at the point at which the Fermi surface just touches the Brillouin zone boundary (see figure 1). One of the first band-structure features noted [8, 9] about the new high- T_c superconductors was that the Fermi surface of the Cu–O₂ plane in LSCO lies almost exactly at the van Hove singularity when $x = 0.15$,

† Also at: Department of Physics, Boston University, Boston, MA 02215, USA.

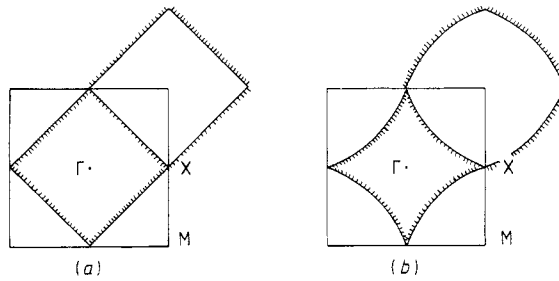


Figure 1. Brillouin zone, with Fermi surfaces, for $\text{La}_{2-x}\text{Sr}_x\text{CuO}_4$, showing simultaneous interpretation as hole surface at M or electron surface at Γ (shading indicates side of Fermi surface occupied by electrons). (a) $x = 0$ (corresponding to $\hat{t} = 0$ in equation (1)). (b) $x = 0.15$ ($\hat{t} = -0.34$).

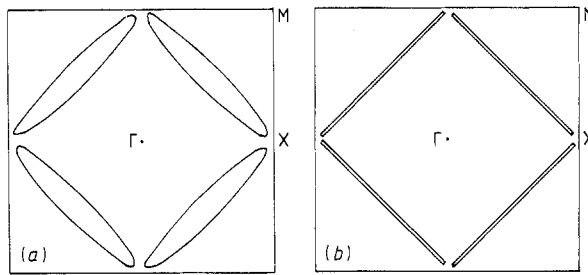


Figure 2. Brillouin zones appropriate to $x = 0.15$: (a) the Fermi-surface sections remaining at the van Hove singularity after the charge- (or spin-) density-wave formation; (b) the regions of k -space occupied by self-trapped holes, after reference [50].

and it was proposed that this feature plays a fundamental role in the superconductivity [9, 10]. Interest in this picture died down when it was found that some of its predictions (e.g., a Peierls transition due to Fermi-surface nesting) were not experimentally observed. Nevertheless, the idealised, quasi-one-dimensional (1D) band structure of figure 1(a) continues to underlie many models of high- T_c superconductivity.

In the first part of the present paper, the experimental and (band-structure) theoretical status of the van Hove singularity is analysed. It is shown that this feature always is found close to the Fermi level of these superconducting oxides, including the new Bi compounds. However, the idealised model of figure 1(a) is inaccurate. The true Fermi surface has considerable curvature, as in figure 1(b). This difference, while subtle, has profound consequences for high- T_c superconductivity. For instance, the Fermi surfaces of figure 1(a) show perfect nesting, leading to a period-doubling Peierls transition which would completely gap the Fermi surface, leaving an insulating ground state. The tendency to instability is greatly reduced with the Fermi surfaces of figure 1(b), and the distorted material remains metallic, with ungapped Fermi-surface sections (figure 2(a)).

This fact suggests a natural separation of the carriers into two groups: a high-density-of-states (DOS) region near the Brillouin zone boundaries, and a low-DOS region over the rest of the Brillouin zone. These carriers can for simplicity be called heavy and light holes, respectively. It is the contention of this paper that this separation into two groups of carriers is essential for understanding high- T_c superconductivity. In simplest terms, it is the light holes which condense, while the heavy holes produce the pairing.

In more detail, the picture is as follows. The heavy holes have strong Fermi-surface nesting, and can be considered as quasi-1D. There is a logarithmic divergence in their

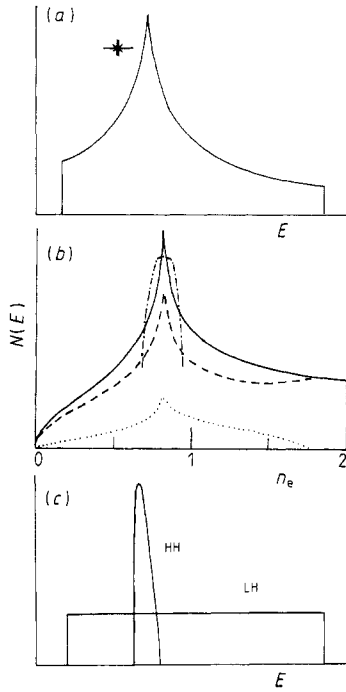


Figure 3. Comparison of density of states for two-dimensional band with van Hove singularity of (a) and (b) with Bilbro-McMillan-type model of Cu-O₂ band (c). Part (a) corresponds to equation (1) with $\hat{t} = -0.34$. The error bars show 20 meV, which is an upper limit to the DOS broadening expected from disorder and 3D coupling. Part (b) represents a numerical solution to the antibonding band of equation (A.1), with $\Delta E = 0.09$, $t_{\text{CuO}} = 0.3$ and $t_{\text{OO}} = 0.1$. The DOS is plotted against $n_e = 1 - x$, the number of electrons per unit cell. The broken and dotted curves are the partial DOS associated with Cu and O, respectively, while the chain curve represents an effective DOS derived from experiments on LSCO (reference [48]). Part (c) shows a schematic separation of the DOS into heavy-hole (HH) and light-hole (LH) contributions.

DOS (figure 3(a)), with similar anomalies in their various susceptibilities. Hence, they are subject to the well known instabilities of the 1D electron gas [11] toward either charge-density-wave (CDW) or spin-density-wave (SDW) formation or singlet or triplet superconductivity. With the Fermi surfaces of figure 1(a) there are only heavy holes, and high- T_c superconductivity would require that the superconducting instability is the strongest—an unlikely possibility. The presence of light holes opens up a new possibility. The heavy holes can have a (spin or charge) density wave (DW) instability, and electronic excitations across the resulting DW gap can produce an additional (excitonic) pairing interaction for the remaining light holes. This model suffers from the original objection: no DW is observed in most of these materials. The present paper shows that this is compatible with reduced dimensionality in these materials. All that is required is short-ranged DW fluctuations, not full long-range DW order. There is abundant evidence that such fluctuations are actually present in the high- T_c materials. Moreover, there is a well developed CDW in BaPb_{1-x}Bi_xO₃ (BPBO), the most three-dimensional (3D) member of the family.

One advantage of this particular model is that it suggests a natural link between superconductivity in the high- T_c oxides and in other groups of materials which display high- T_c or other unusual superconducting properties, including the A15s, heavy fermions and organic superconductors. In the A15s there are high-DOS, quasi-1D sections of the Fermi surface coexisting with low-DOS regions, and there is a competition between superconductivity and a structural instability. The highest T_c s occur just before the structural transition, when all the carriers can participate in superconductivity. In these 3D materials, the CDW gap may be too large to produce significant excitonic pairing.

The present paper describes this new model in broad outline. A companion paper (paper II) [12] shows that the proposed mechanism can indeed produce T_c s in the observed range. Some brief accounts of this work have already appeared [13, 14]. The

outline of this paper is as follows. Section 2.1 and the appendix present a simple tight-binding model for the Cu–O₂ bands, showing that the curved Fermi surfaces of figure 1(b) are associated with direct O–O hopping. Section 2.2 provides experimental and (band-structure) theoretical evidence for the near coincidence of Fermi surface and van Hove singularity in the new superconducting oxides. Section 3 presents the model for excitonic superconductivity in the presence of either long-range (§ 3.1) or short-range (§ 3.2) DW order. Section 4 discusses a number of salient features associated with the model. In particular, since the van Hove singularity is associated with a fixed carrier density, the occurrence of superconductivity over an extended doping range in LSCO is understandable only if the compounds are a two-phase mix, with one phase at the van Hove point. The reasons for this phase separation are discussed in § 4.1. Section 4.2 discusses the DW in more detail; § 4.3 suggests why T_c is higher in YBCO and the Tl and Bi compounds; § 4.4 discusses deviations from two-dimensionality, § 4.5 the isotope effect and § 4.6 the comparison with other excitonic theories. Section 5 summarises the main conclusions, while § 6 suggests a deeper interpretation of the underlying physics.

2. Role of the van Hove singularity

2.1. Model band structure

The calculation is restricted to the antibonding Cu–O band of the CuO₂ planes. The essential physics is contained in the following model two-dimensional (2D) band structure [15]:

$$\varepsilon_k = -2t_0(\cos k_x a + \cos k_y a + \hat{t} \cos k_x a \cos k_y a) \quad (1)$$

where $E_B = 8t_0$ is the full bandwidth.

Equation (1) can be derived from a tight-binding Hamiltonian:

$$H = E_{\text{Cu}} \sum c_{i\sigma}^+ c_{i\sigma} + E_{\text{O}} \sum a_{i\sigma}^+ a_{i\sigma} + t_{\text{CuO}} \sum (a_{i+\delta,\sigma}^+ c_{i\sigma} + \text{HC}) \\ + t_{\text{OO}} \sum (a_{i+\delta',\sigma}^+ a_{i\sigma} + \text{HC}) \quad (2)$$

where the sums are over lattice sites (i), spins (σ) and nearest neighbours (δ, δ'), and HC stands for Hermitean conjugate.

The band structure corresponding to equation (2) is analysed in the appendix. The results depend on the relative values of the hopping integrals and $\Delta E \equiv E_{\text{Cu}} - E_{\text{O}}$. When $\Delta E \gg t_{\text{CuO}}$ and t_{OO} , the antibonding band is of the form of equation (1), with

$$t_0 = 2t_{\text{CuO}}^2/\Delta E \quad (3a)$$

$$\hat{t} = -4t_{\text{OO}}/\Delta E. \quad (3b)$$

In the oxide superconductors, the opposite limit is more likely to apply, $\Delta E \ll t_{\text{CuO}}$ and t_{OO} . In this case, as shown in the appendix, the expression for the energy bands is more complicated than equation (1). However the qualitative features, in particular the shapes of the Fermi surfaces and the role of t_{OO} , are quite similar. For instance, figure 3(a) shows the DOS associated with equation (1) (large ΔE), and figure 3(b) shows that calculated numerically for the antibonding band of equation (A.1) for a situation with small ΔE .

Equation (1), with $\hat{t} = 0$, is the familiar tight-binding form used in many previous high- T_c calculations. When \hat{t} is neglected, the half-filled band (figure 1(a)) has a square

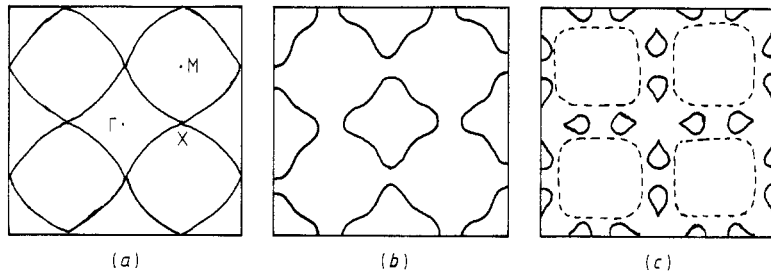


Figure 4. Fermi surfaces derived from positron annihilation studies: (a) after reference [19], (b) and (c) after reference [20]. (b) Raw data, figure 3 of reference [20]; (c) analysed into a superposition of two Fermi surfaces (broken and full curves), figure 5 of reference [20]. See discussion in text.

Fermi surface and hence perfect nesting, leading to very singular behaviour. Inclusion of \hat{t} produces more rounded Fermi surfaces, greatly reducing the nesting and the strength of the singularity and shifts the nesting condition away from the half-filled band. The importance of direct O–O hops has also been noted by Stechel and Jennison [16], and Yu *et al* [17] have shown that both terms of equation (1) are necessary to describe correctly their calculated Fermi surfaces for YBCO and $\text{Ti}_2\text{Ba}_2\text{Ca}_n\text{Cu}_{n+1}\text{O}_{2n+6}$, $n = 1, 2$ (TBCCO).

There is high-DOS region associated with the van Hove singularity of the 2D energy bands—the saddle-point energy at which conduction crosses over from electron-like to hole-like. The high-DOS regions occur near the X points in figure 1, where the Fermi surface intersects the Brillouin-zone boundary. For purely 2D bands, the DOS is logarithmically infinite at this energy. In reality, the singularity is smeared out by interlayer coupling and finite carrier lifetime. In § 4.4 it is shown that these effects are relatively small, and still allow a well defined separation of light and heavy holes. For the present purposes, the logarithmic DOS (figures 3(a) and (b)) is not essential, and the DOS may be approximated by the non-singular form of figure 3(c).

If \hat{t} is negative, the van Hove singularity occurs at the Fermi energy E_F when the CuO_2 planes are positively doped. For instance, the singularity falls at the Fermi level of LSCO of optimum T_c ($x = 0.15$) for $\hat{t} = -0.34$. This negative value of \hat{t} is consistent with a naive model of treating the hybridised Cu–O₂ bands as an isolated unit (as in the appendix). In this case it might be expected that the most nearly-free-electron-like behaviour (circular Fermi surfaces) would occur at the bottom of the bonding and the top of the antibonding bands. This is true only if $\hat{t} < 0$.

2.2. Evidence for the van Hove singularity

In local-density band-structure calculations for LSCO [8, 9] and in 2D calculations for YBCO [18], the Fermi surface is located at the van Hove singularity. This appears to be the case also for full 3D calculations in YBCO, but in this case a nearly degenerate Cu–O chain band overlaps and hybridises with the Cu–O₂ plane band, thereby complicating the interpretation. The hybridisation can be nicely illustrated by a careful analysis of recent *experimental* positron annihilation results [19, 20] (figure 4) which appear to capture the principal features of the band-structure analysis.

Figure 4(a) shows the relevant Fermi-surface section found by Peter's group [19]. The raw 2D ACAR data (maximum gradient of carrier momentum) found by Smedskjaer *et al* [20] look very similar (figure 4(b))—the technique is not sensitive to the nearly localised carriers near the X points. However, 'with guidance from theory', these data

were analysed as a superposition of the two Fermi–surface sections shown in figure 4(c). The Fermi surface of figures 4(a) and (b) clearly agrees with the model of figure 1(b) and the 2D calculation of reference [18]. That of figure 4(c) shows the modifications introduced by the Cu–O chains. The present model requires only high-DOS and low-DOS regions of Fermi surface, and hence is insensitive to these modifications of the Fermi surface. The presence of two types of low-DOS carriers, one associated with the chains and one with the planes, may, however, explain some other properties of YBCO, such as the anomalous temperature dependence of the Hall coefficient [21], and may be essential in enhancing T_c , as discussed below.

A similar situation arises in the newer Bi and Tl superconductors. In $\text{Bi}_2\text{Sr}_2\text{CaCu}_2\text{O}_x$, the Fermi level falls very close to a van Hove singularity at the X point (figure 2 of reference [22]). The same general shape of figure 1(b) is clearly seen in the calculated Fermi surfaces (figure 3 of reference [23]), but the region near the X points is severely distorted by an additional Fermi-surface pocket due to Bi–O states.

It should be cautioned, however, that while the general agreement between positron annihilation studies [19, 20] and band-structure calculations is good for YBCO, there have been questions raised about the accuracy of band-structure calculations in describing these materials. In particular, it is found that local-density calculations cannot explain the antiferromagnetic insulating ground state of La_2CuO_4 [24]. The strong correlation effects make any one-electron band structure somewhat suspect. Much more significant are the photoemission experiments, discussed below, which provide strong support for the picture of heavy and light holes at E_F .

Further experimental evidence for light and heavy holes comes from normal-state transport measurements. The large resistivity, linear in T , is due to electron–electron scattering involving the heavy holes [25], whereas Hall-effect measurements [26] see only a low carrier density consistent with the light holes (figure 2(a)). This can easily be understood as a mobility effect. A simple two-band calculation shows that if the heavy-hole mobility is only $\frac{1}{3}$ as high as that of the light holes, the heavy holes will produce only a 20% increase in the Hall coefficient, R_H . The weak temperature dependence of R_H in LSCO could be due to a gradual heavy-hole freeze-out as short-range DW order grows.

Finally, recent photoemission experiments [27] are consistent with a small density of mobile carriers plus a high density of nearly localised carriers at the Fermi level, if allowance is made for final-state effects. The measured photoemission spectrum (figure 5(a)) shows a number of sharp features associated with nearly localised charges, plus a delocalised continuum which produces a well defined step at the Fermi level (figure 5(a), inset). In interpreting the localised features, the presence of the final-state hole must be taken into account, leading to the assignments of figure 5(b). From this assignment, the positions of the localised bands in the absence of final-state holes may be inferred by a cluster calculation. As shown in figure 5(d), hybridisation effects produce a large additional splitting of the Cu d hole ($3d^9$), and the O 2p hole ($3d^{10}\underline{L}$) features. The sharp structure at the Fermi level is thus the predominantly $3d^9$ state, nearly localised, while the continuum background is due to hybridisation with the more extended O 2p states. Figure 5(c) should be compared with figure 3(b). The small additional splitting of the $3d^9$ level, due to the CDW, amounts only 0.4 eV and would be difficult to detect in photoemission.

Summarising, it can be noted that both experiment and band-structure calculations are consistent with a picture of the van Hove singularity occurring near the Fermi level. Even at room temperature, the strong scattering associated with the singularity ensures that the high-DOS holes are nearly localised (large short-range DW order). It should be

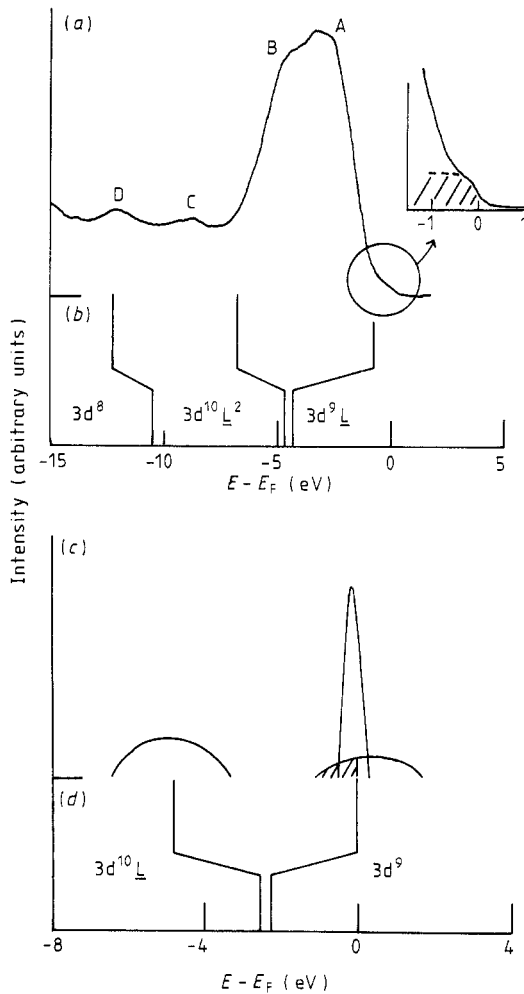


Figure 5. Analysis of x-ray photoemission data for $\text{La}_{1.8}\text{Sr}_{0.2}\text{CuO}_4$, after Shen *et al* [27]. (a) Photoemission spectrum, showing sharp features A–D corresponding to nearly localised charges, plus a continuum feature near the Fermi level E_F (shaded part of inset). (b) Interpretation of features A, B and D in terms of valence-band hole states (see reference [27] for a discussion of feature C). Lower lines are bare energies, upper lines include hybridisation. (c) Ground-state energy bands inferred from (a) and (b). The O 2p band is assumed to have a larger width due to direct O–O hopping. (d) Ground-state energy levels, as in (b).

stressed that, in the absence of heavy-hole localisation, the small measured Hall-effect carrier densities are incompatible with the Fermi surfaces found in band-structure calculations.

3. Model for superconductivity

3.1. Excitonic superconductivity

Given the separation of the carriers into heavy and light holes, a close similarity between the high- T_c oxides and the A15 superconductors becomes apparent. These compounds can be thought of as a 3D array of interpenetrating conducting chains. Hence there are quasi-1D sections of Fermi surface, and early theories suggested that the CDW and superconducting instability were associated with the 1D DOS singularities. However, Bilbro and McMillan [28] (BM) showed that the competition between superconductivity and CDWs can be adequately described by fully three-dimensional energy bands, as long as the carriers fall into two groups, associated with high-DOS and low-DOS.

The high-DOS carriers in the A15s are also associated with parts of the Fermi surface near the X points, and also have significant nesting, which leads to a competition between

superconductivity and CDW formation. By a slight modification, the theory can also describe a system with a SDW instability [29]. In the CDW phase, the peak in the DOS is split into two peaks, one driven a distance $W(T)$ below the Fermi level, the other above. It is this lowering of the energy of the occupied peak which stabilises the CDW. If the CDW transition does not occur, a superconducting transition can take place with a relatively high T_c , because of the large total DOS. Once the CDW transition sets in, superconductivity will involve gapping only the light holes, with considerably smaller DOS and hence much lower T_c . The competition between these two interactions explains why superconductivity in the A15 compounds is located very close to a structural instability, and why it is so difficult to optimise T_c in these materials.

BM developed a simple model of the A15s to account for this competition. Their model has already been used [30] to interpret the superconductivity of BPBO, which has a long-range CDW transition. The BM Hamiltonian has also been applied to LSCO [31], identifying the CDW transition with the tetragonal–orthorhombic (TO) transition. However, from the known distortions of the oxygen atoms, it is presently believed that the TO transition does not open a gap at the Fermi level [32]. Moreover, a purely phonon-induced pairing interaction would probably overestimate the isotope effect in this material [3], and cannot explain the very high T_c s found in YBCO or the new Tl and Bi compounds.

Hence, a new mechanism for pairing is needed. In the context of a BM-like model, there is one obvious candidate: the DW gap itself. This is the lowest electronic gap in the system, and hence the most likely source of an excitonic pairing [33, 34]. In paper II a detailed dielectric constant calculation is provided, showing that this mechanism can lead to T_c s of the appropriate magnitude. Here, however, I introduce a modified BM Hamiltonian which allows a convenient generalisation to include DW fluctuations.

In the BM model, energy space is divided into region 1, corresponding to the high-DOS carriers, and region-2, for the low-DOS carriers. Two electron–phonon coupling parameters are introduced, V_P driving the Peierls (CDW) transition and V_{BCS} providing the superconducting pairing. These lead to coupled equations for the CDW gap W and the BCS gap Δ :

$$W = V_P \int_1 d\varepsilon \rho_1(\varepsilon) \frac{W}{2\Omega_1(\varepsilon)} \tanh \frac{\Omega_1(\varepsilon)}{2k_B T} \quad (4)$$

$$\Delta = V_{BCS} \sum_l \int_{-\hbar\omega_0}^{\hbar\omega_0} d\varepsilon \rho_l(\varepsilon) \frac{\Delta(\varepsilon)}{2\Omega_l(\varepsilon)} \tanh \frac{\Omega_l(\varepsilon)}{2k_B T} \quad (5)$$

where \int_1 is an integral over region 1,

$$\Omega_l^2 = \varepsilon^2 + \Delta^2(\varepsilon) + W^2 \delta_{l1} \quad l = 1, 2 \quad (6)$$

$$\Delta(\varepsilon) = \begin{cases} \Delta & |\varepsilon| < \hbar\omega_0 \\ 0 & |\varepsilon| > \hbar\omega_0. \end{cases} \quad (7)$$

ω_0 is a characteristic phonon energy and ρ_l is the DOS. Away from the van Hove singularity, the DOS may be considered constant, $\rho_2(\varepsilon) \approx N_2$; however, in region 1, ρ_1 has a strong energy dependence. In the 2D limit, $\rho_1(\varepsilon) = N_1 \ln(t_0/|\varepsilon|)$, with $N_1 = 2/(\pi t_0 V_0)$, and V_0 is the unit cell volume. When $\Delta = 0$, BM reduces to a purely CDW transition, and $W(T)$ has the BCS form if the DOS in region 1 is constant. Including the logarithmic singularity produces large deviations from BCS form.

Since the excitonic coupling has the same BCS form as ordinary phonon coupling, it can be incorporated in the BM model by adding a second term to the right-hand side of

equation (5), of the same form but with the substitutions $V_{\text{BCS}} \rightarrow V_x$, the exciton pairing potential, and $\hbar\omega_0 \rightarrow W(T)$, the CDW gap. When exciton coupling is dominant, the phonon contribution to equation (5) may be ignored. Since W has a non-BCS temperature dependence, the resulting $\Delta(T)$ will have a very non-BCS form, and $2\Delta(0)$ can be much greater than $k_B T_c$. A typical example is given in reference [14].

3.2. Short coherence length limit

The above model for the CDW is expected to be valid when the temperature dependence is dominated by electron entropy. In the high- T_c superconductors the opposite limit, phonon-entropy dominant, is likely to be more important. This is because the number of phonon modes involved is large when the electronic coherence length ξ is small—all phonons with wavenumber within ξ^{-1} of the soft mode are important. This excess entropy depresses the CDW transition temperature, while fluctuation effects and short-range order are important at high temperatures. In the extremely short coherence length limit, the electron entropy may be ignored.

For the case of the pure CDW ($V_{\text{BCS}} = V_x = 0$), a simple mean-field calculation has been carried out by McMillan [35], and may be briefly summarised. The order parameters are averages over phonon amplitudes, the long-range order parameter $\langle \psi \rangle \propto W$, and the short-range parameter $\langle |\psi|^2 \rangle$. $\langle \psi \rangle$ is proportional to the mean static lattice displacement, $\langle |\psi|^2 \rangle$ to the mean-square local lattice displacement or local energy gap. At this point, it would be premature to distinguish commensurate and incommensurate CDW phases, and only the incommensurate phase will be considered. The equilibrium values of $\langle \psi \rangle$ and $\langle |\psi|^2 \rangle$ are found by minimising the (normalised) free energy:

$$F = \frac{4}{\pi^2} \langle \psi \rangle^2 - \frac{D'}{C} \langle |\psi|^2 \rangle^2 - t \ln \int d^2 \psi \exp(-V_1(\psi)/t) \quad (8)$$

with potential

$$V_1(\psi) = (A'/C + \nu + 4/\pi^2) |\psi|^2 - (8/\pi^2) \text{Re}(\psi^* \langle \psi \rangle) + (2D'/C) |\psi|^2 \langle |\psi|^2 \rangle. \quad (9)$$

In the above equations C , A' and D' are constants which fix the energy scales for the electronic energy, elastic energy and CDW interaction respectively, while $t = T/T^*$ is a normalised temperature. The temperature T^* depends on microscopic parameters and is proportional to ξ^2 . The electronic term ν depends on the form assumed for the DOS. McMillan [35] used a constant DOS, $\rho_1 = N_1$, for which $\nu = \ln |\psi|^2$. If $\rho_1 = N_1 \ln(t_0/\varepsilon)$, then $\nu = \ln^2 |\psi|^2 / 8$. Figure 6 compares the temperature dependence of the order parameters for these two choices of DOS.

Incorporation of excitonic superconductivity is then straightforward, as in equation (5). There is no necessity for the bosons which produce Cooper pairing to be long-lived, so the superconducting gap should be a function of the short-range order parameter, $W_s \propto \sqrt{\langle |\psi|^2 \rangle}$. Hence, superconductivity can arise without the appearance of a long-ranged CDW phase. The resulting gap $\Delta(T)$ (figure 7) shows deviation from BCS form, particularly in having a stronger temperature dependence at low T . For the parameters chosen in figure 7, $2\Delta/k_B T_c = 4.85$.

4. Discussion

Any new model which seeks to explain high- T_c superconductivity must raise a great number of questions as to how it accords with experiment. In this section, a number of these issues are discussed.

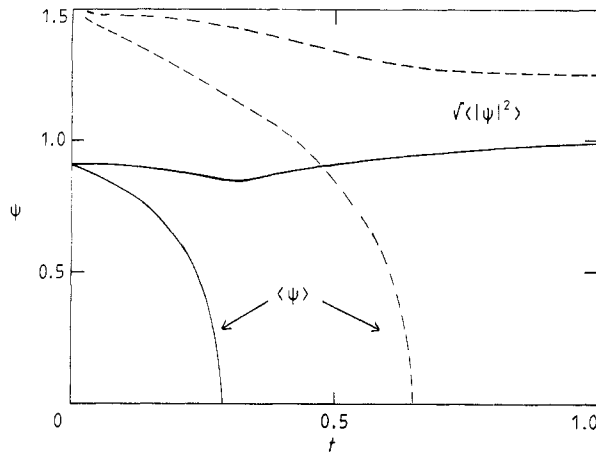


Figure 6. Short-correlation-length CDW, showing both long-range ($\langle \psi \rangle$) and short-range ($\sqrt{\langle |\psi|^2 \rangle}$) order parameters in the McMillan model, assuming $A'/C = -0.965$, $D'/C = 0.2$. Full curves represent constant DOS, broken curves represent logarithmic DOS.

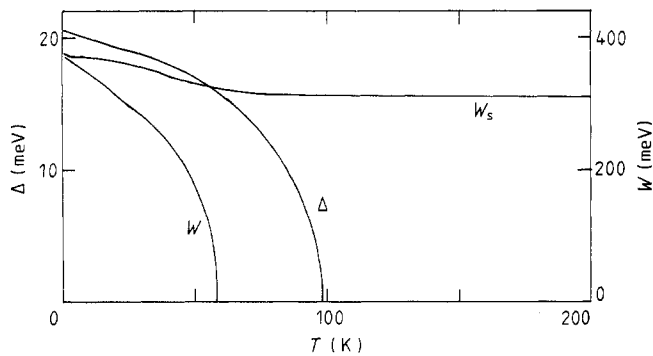


Figure 7. Excitonic superconductivity in the short-correlation-length model. The calculations assume the parameters of figure 6 (log DOS), $W/\langle \psi \rangle = 250$ meV, $T^* = 7.8$ meV and $\lambda_3 = 0.29$.

4.1. $\text{La}_{2-x}\text{Sr}_x\text{CuO}_4$: a two-phase system

LSCO presents a special challenge to any theory based on the van Hove singularity, because superconductivity persists over an extended range of hole concentration, for x between 0.04 and 0.3. This is possible only if the Fermi surface is pinned at the van Hove singularity. If this naturally occurs for some x_0 (where $x_0 \approx 0.15$ –0.2), then for $x \neq x_0$, the material must occur in a two-phase mixture [15], with one phase at x_0 and the other at some other stable phase, for example near $x = 0$ (La_2CuO_4). The phases could be purely electronic, or could involve some atomic rearrangements. Since a short-range diffusion of Sr or O would cost relatively little energy while maintaining charge neutrality, a spinodal decomposition might occur in these systems [15]. The purely electronic instability would be very similar to the ferron phase in a semimagnetic semiconductor [36].

Why does such a phase separation occur? It has been proposed [37, 38] that this is a 2D analogue of a Hume-Rothery phase [39], in which strong electron–phonon coupling induces a lattice instability near the carrier concentration at which the Fermi surface just

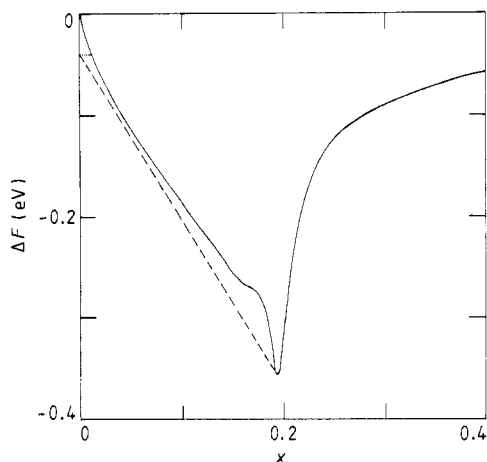


Figure 8. Hole free energy ΔF against doping x for $\text{La}_{2-x}\text{Sr}_x\text{CuO}_4$. Calculation includes on-site Coulomb repulsion and electron-phonon coupling. The full curve (calculated) is the correlated Fermi liquid; the dotted curve (schematic) is the antiferromagnetic insulator. The broken line indicates the two-phase coexistence region (reference [38]).

spans the Brillouin zone. In the present oxides, the susceptibility anomaly associated with the van Hove singularity greatly enhances the likelihood of a Hume-Rothery phase (which may incidentally explain why these materials are so easy to fabricate). Figure 8 shows a model free-energy diagram [38] for LSCO, incorporating both the standard electron-phonon coupling used in 3D studies of Hume-Rothery phases [40] and an electron-electron interaction (on-site Coulomb repulsion) [41], to stabilise the Mott phase near $x = 0$ (see below). It clearly illustrates the two-phase nature of the system for $x \neq 0, x_0$.

The experimental evidence of this phase separation provides the clearest evidence of the important role played by the van Hove singularity. This evidence is somewhat ambiguous because of the system complexity. A second phase might arise from, for example, variations in oxygen stoichiometry and be mistaken as evidence for this phase separation. On the other hand, spinodal decomposition may have very slow kinetics at low temperatures, and a metastable homogeneous phase can easily be quenched in. Nevertheless, there is considerable evidence for two phases (whether electronic or compositional) in the LSCO compounds with $x \neq 0.15$. (The situation in YBCO is much more complicated: variations in oxygen stoichiometry can give rise to a series of intermediate phases). Thus, Hinks *et al* [42] reported that LSCO with $x > 0.15$ is a two-phase mixture of $\text{La}_{1.85}\text{Sr}_{0.15}\text{CuO}_4$ and $\text{La}_2\text{SrCu}_2\text{O}_6$, but that a metastable homogeneous state can easily be quenched in; van Dover *et al* [43] suggested that, based on Meissner fraction measurements, LSCO is single-phase only near $x = 0.15$, and is two-phase for x either greater or less than this value; the original study [44] of T_c as a function of x shows evidence for two resistive transitions in samples with x far from 0.15, and Venturini [45] has found great difficulty in preparing single-phase compositions for $0.04 \leq x \leq 0.1$. Uher and Kaiser [46] found evidence for isolated superconducting inclusions at low x values, for which the sample resistivity never goes to zero, and small traces of a superconducting phase are found even near $x = 0$ [47]. Finally, a recent study [48] has confirmed that T_c is optimised near $x = 0.2$.

Normal-state transport in LSCO can also be understood in terms of this two-phase model. Figure 9 shows that the doping dependence of the Hall coefficient and resistivity [26] can be described by an effective-medium theory [49], assuming pure phases at $x = 0, 0.15$ and 0.2 . Moreover, using data for $x = 0.10$ and 0.15 only, the effective-medium theory can be extrapolated to predict the resistivity of pure La_2CuO_4 , in good agreement with other experiments [14].

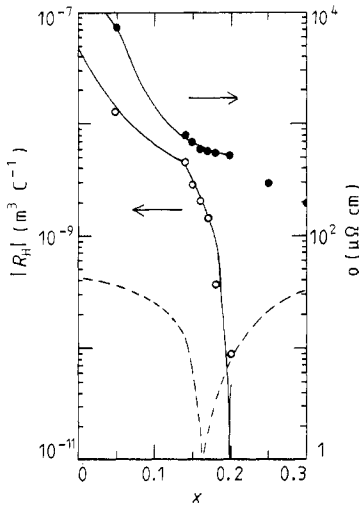


Figure 9. Hall coefficient (open circles) and resistivity (full circles) against x ; data from reference [26]. Full curves show two-phase effective medium theory; broken curve shows single phase ($= -R_H$ for $x > 0.19$).

The nature of the phase at $x = 0$ is quite interesting. It appears to be a Mott insulator, due to strong on-site Coulomb repulsion (dotted line in figure 8). The usual picture of the Mott transition is that it is driven by extremely strong correlation effects associated with a half-filled band: the electrons can greatly lower their Coulomb energy if no two electrons ever occupy the same atom. In the present system, these correlation effects act to increase the separation between the Cu and O energy levels, ΔE [41]. The effect of this renormalisation can readily be seen from equation (3). Not only is the bandwidth reduced ($t_0 \rightarrow 0$), but band-structure effects are washed out ($\hat{t} \rightarrow 0$) and the van Hove singularity is pushed towards the half-filled case. Thus, in LSCO, the Fermi surface of figure 1(b) is appropriate for the doped material ($x = 0.15$) and that of figure 1(a) for the undoped ($x = 0$). In the latter case, the greatly reduced bandwidth and enhanced nesting ensure that a SDW transition will occur at a relatively high temperature.

Near the van Hove singularity ($x \approx 0.15$), the effects of correlations are much weaker, particularly when direct O–O hopping is allowed ($t_{OO} \neq 0$). This is clearly illustrated in the calculations of reference [38] (figure 8), where a slave boson technique [41] is used to incorporate on-site Coulomb repulsion, while the electron–phonon interactions responsible for Hume-Rothery phase separation are simultaneously included.

Because of the two-phase coexistence regime and the fact that band-structure information is lost in the AFM phase, extrapolating from the AFM phase to understand the high- T_c phase is extremely problematic. In particular, the AFM phase is the same in the high- T_c oxides and the magnetic semiconductors, so whether doping produces a high- T_c superconductor or a ferron phase [36] depends entirely on the properties of the second phase. Some recent studies [50, 51] have found that, just as in the magnetic semiconductors, excess holes added to the AFM state are self-trapped, and pairs of holes attract. I would interpret this as the first stage of the phase separation. Zaanen *et al* [24] have shown that multi-hole clusters are also stable. The self-trapped holes [50] are localised in k space near the initial Fermi surface (figure 1(a)). This gives them a momentum-space distribution (figure 2(b)) which is very similar to the Fermi surfaces of the light holes, after the CDW transition (figure 2(a)).

4.2. The density wave

A number of questions about the short-range DW fluctuations remain unanswered. Do SDW or CDW fluctuations predominate? Is there a transition to long-range DW order, and

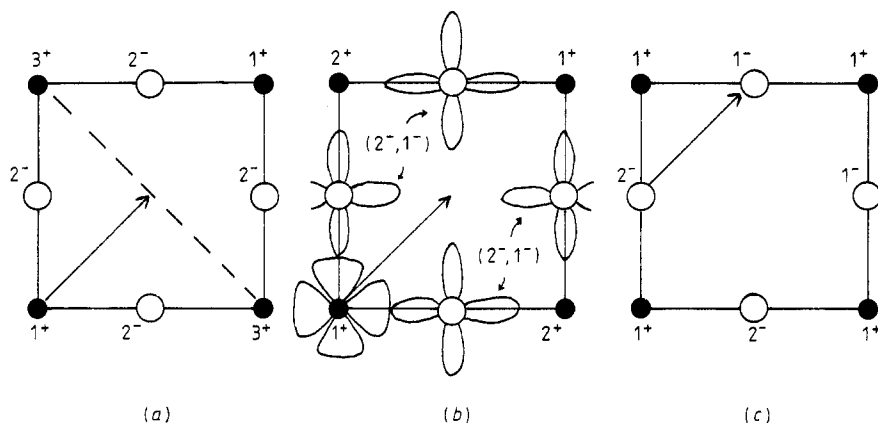


Figure 10. Possible models of CDW formation. Full circles are Cu, open circles are O. The arrow shows the charge separation vector. (a) Cu valency alternation; (b) charge transfer exciton; (c) modification of (b) with O-valence alternation. In (b) the lobes of the Cu 3d and O 2p orbitals are shown.

does it occur above or below the superconducting transition? The present section provides some possibilities, without reaching any firm conclusions.

It is perhaps useful to look first at La_2CuO_4 . Here strong 2D spin-density correlations are present for hundreds of degrees above the AFM transition [52] (which may be considered as a commensurate SDW). This occurs because long-range order cannot exist in a strictly 2D system: the AFM transition is driven by extremely weak interlayer correlations. These SDW fluctuations persist into doped LSCO at least to $x = 0.12$, even though the AFM Néel temperature is depressed strongly with increasing x , going to zero above $x \approx 0.4$. Could these fluctuations persist out to $x = x_0$, and be responsible for the excitonic pairing?

I think that, instead, the relevant fluctuations are of a CDW, strongly coupled to lattice vibrations. Certainly, there is a well defined CDW in BPBO, the most 3D of the superconducting oxides. Moreover, in both LSCO and YBCO there seems to be anti-correlation between superconductivity and the AFM state, as would be suggested by figure 8. An analogous situation arises in the theory of 1D metals [53]. SDW fluctuations may dominate at high temperatures, but when interchain coupling is strong, the dominant low-temperature instability is a CDW.

DW fluctuations must be present even at room temperature, since the optical excitonic feature is observed at these temperatures. A similar situation occurs in the pure CDW state in 2H-TaSe_2 , where the energy gap is $0.3 \text{ eV} \sim 24k_B T_{\text{CDW}}$. In fact, McMillan's short-coherence-length theory [35], discussed in § 3.2, was designed to describe this material.

The question is, when does long-range order set in? It is possible that the CDW is associated with the structural transitions which have been observed just above T_c [54]. Alternatively, the transition to long-range CDW order may not occur at all for $T > T_c$. There is considerable evidence [55] of anomalies in phonon-related properties at or slightly above T_c , which suggest a CDW. However, this evidence must be treated cautiously, since the phenomena could be generated indirectly. Superconductivity will reduce ordinary scattering of phonons by electrons, and hence modify virtually all phonon properties, regardless of the mechanism of superconductivity.

The present considerations cannot specify the exact form of the CDW distortion. All that is required is that the distortion splits the van Hove singularity. Figure 10 presents

some possible CDW distortions which are consistent with this requirement. The simplest picture is that the CDW causes a Cu^{1+} – Cu^{3+} valence alternation (figure 10(a)). This is a two-dimensional version of the CDW in BPBO. However, photoemission studies reveal the absence of Cu^{3+} ; the extra holes preferring to go on the oxygen, producing O^{1-} . Modifying figure 10(a) so that the hole is shared by the four oxygens surrounding the original Cu^{3+} gives the alternate CDW of figure 10(b). Note that, for charge conservation, the actual electronic wavefunction on the oxygens must be a mixture of O^{2-} and O^{1-} states. In figure 10(b), only half of the Cu^{2+} convert to Cu^{1+} . Mazumdar [56] has suggested another possibility: all of the Cu^{2+} converts to Cu^{1+} , so that (in the absence of doping) half of the O^{2-} become O^{1-} to preserve charge neutrality. An ordering of the O^{1-} – O^{2-} ions would then restore the symmetry of the problem. Figure 10(c) shows one such ordering (this is not identical to the ordering suggested by Mazumdar). In all of these cases, figure 10 shows intralayer correlations only. The strong, weakly screened Coulomb interactions along the c axis could lead to a more complicated three-dimensional order. If the recent reports of ‘oxygen dimers’ [57] can be confirmed, they would be likely candidates for DW fluctuations.

Why are the excitonic effects so much weaker in the A15 compounds, which have well defined CDWs? It may be that the CDW gap is too big to promote superconductivity [12]. Just as in phonon-induced pairing, excitonic attraction wins out over electron–electron repulsion because of retardation effects. The first hole polarises the excitonic background, the second is attracted to this polarisation after the first hole has passed. This requires that the excitonic frequency be small compared with electronic frequencies, or equivalently, $2W \ll E_B$, the electronic bandwidth. To account for retardation effects, the integral on the excitonic term of equation (5) should be cut off when W is larger than $\sim E_B/5$. In the high- T_c oxides, W is approximately of this order of magnitude. In other CDW systems, W may be $\gg E_B$, in which case the excitonic contribution is unimportant.

4.3. Why is T_c higher in YBCO and the newer Bi and Tl compounds?

In LSCO, both the excitons and the superconducting holes arise from the same band of CuO_2 -plane holes. This is distinct from Little’s original excitonic concept [33], when one group of localised electrons produced the polarisation, pairing carriers which belonged to a totally different group. Such an effect could occur in YBCO: the higher T_c would be due to the fact that there are two groups of superconducting carriers, light holes from the CuO_2 planes and carriers from the CuO chains. This would explain why, when the chains are disrupted, T_c drops to ~ 60 K [58], nearly the same value as for LSCO under pressure.

A similar effect could also occur in the Tl and Bi compounds. The pure CaCuO_2 compound is insulating [59], that is, it requires doping of the CuO_2 planes to move the Fermi level to the van Hove singularity. The high T_c s of the Tl and Bi compounds must arise in part because of this charge transfer, but there are also free carriers in the Tl–O or Bi–O layers, which can be paired just as in YBCO.

Allender *et al* [34] have suggested that T_c could be raised even further at the interface of two appropriate materials, for example a metal film on a semiconductor. In a sense, the Bi and Tl compounds may already be an example of this, with metallic layers intercalated between CuO_2 sheets. Such an effect could also occur in these high- T_c oxides, by preparing an intimate mixture of the excitonic and a metallic phase (high carrier concentration, and hence reduced tendency to CDW formation). This mixture could arise naturally, via spinodal decomposition [14], in these multi-component oxides.

Indeed, the recently observed Bi alloy ‘cryptocrystals’ [60] show that such intimate mixtures can arise in these systems, although it does not appear that, in this instance, the mixture has enhanced T_c . In any case, the very short coherence lengths in these materials require that the two phases be mixed on an extremely fine scale.

4.4. Effects of two-dimensionality

The present model does not inherently require two-dimensionality, only a high-DOS region at the Fermi surface, with a separate group of low-DOS carriers. It may well be that the nearly 2D bands in the superconducting oxides enhance the effectiveness of the mechanism: larger DOS, greater temperature range for DW fluctuations. Nevertheless, there is nothing in the model which requires, for example, the DOS to diverge logarithmically as $T \rightarrow 0$ (unlike some other theories). For actual calculations, however, it is useful to estimate how large the rounding of the DOS is likely to be. These estimates are made in this section.

Since the gap equation already includes thermal smearing, the two features which could wash out the DOS singularity are three-dimensional (3D) coupling and lifetime effects. These will cause smearing of the logarithmic DOS peak over energy scales ΔE_{3D} and ΔE_τ respectively. These energy scales can be estimated as follows:

$$\Delta E_\tau = \hbar/\tau = \hbar n e^2 \rho / m. \quad (10)$$

Taking the light-hole density $n = 3 \times 10^{21} \text{ cm}^{-3}$, the mass m to be the free-electron mass, and the resistivity $\rho = 200 \mu\Omega \text{ cm}$ at T_c , $\Delta E_\tau(T_c) = 11 \text{ meV}$. Since ρ is dependent on temperature, ΔE_τ will be smaller at lower T . The second, T -independent contribution, ΔE_{3D} , must be estimated from band-structure calculations. In these layered materials, a sharp distinction must be drawn between intrasandwich and intersandwich coupling. For instance, TBCCO and related Bi compounds show a staging phenomenon similar to intercalated graphite. A stage number can be defined by the number of CuO_2 layers between successive pairs of Tl layers. Stages 1–3 have all been observed experimentally, with T_c an increasing function of the stage index. In stages 2–3, the Cu layers *between* successive pairs of Tl layers (‘intrasandwich’) can be relatively strongly coupled, whereas Cu layers separated by Tl layers (‘intersandwich’) are very weakly coupled.

The *intrasandwich* coupling will split the DOS peak into several inequivalent peaks (N peaks in stage N). However, each peak will have a logarithmic singularity, and the DW and superconducting transitions will be dominated by the largest peak. (In principle, the more complicated situation of a competition between two peaks is also possible, but will not be discussed further here.) It is only the intersandwich coupling which produces true three-dimensional order and hence rounds off the logarithmic singularity. The strength of this coupling is measured by the intersandwich coupling, or 3D bandwidth, ΔE_{3D} . Calculations show that this dispersion is less than 10 meV [9] in YBCO, and may actually vanish [18, 61]. Hence, a conservative estimate is $\Delta E_{3D} \leq 10 \text{ meV}$, so the total $\Delta E = ((\Delta E_{3D})^2 + (\Delta E_\tau)^2)^{1/2} \leq 15 \text{ meV}$ at all temperatures, and $\Delta E \rightarrow \Delta E_{3D}$ as $T \rightarrow 0$. The error bars in figure 3(a) show a spread of 20 meV. It can be seen that smearing out the DOS on this energy scale would not affect the overall shape of the DOS, but only smear out the immediate vicinity of the peak. Since DOS structure affects the temperature dependence of W or Δ only at very low temperatures, for which $\Delta E \approx \Delta E_{3D}$, a detailed comparison of theory with experiment can fix the value of this poorly known parameter.

In LSCO, there is significant c -axis dispersion because the Γ and Z points alternate one above the other in the tetragonal Brillouin zone [8, 9]. However, this dispersion has

relatively little effect, since it is topologically necessary that the van Hove singularity occurs in the central plane (containing Γ) and the end faces (containing Z) of the Brillouin zone at exactly the same energy level.

Some idea of the broadening of the DOS can be found by analysing the doping dependence of T_c in LSCO. If neither DW formation nor phase separation occurred, there would be a purely phonon-induced superconducting transition, with T_c a sensitive function of the total DOS, N :

$$T_c(x) = T_{c0} \exp(-1/(N(x)V_{BCS})). \quad (11)$$

Assuming T_{c0} and V_{BCS} are independent of x , the data of reference [48] can be used to reconstruct an effective DOS, $N_{\text{eff}}(x)$. This is plotted in figure 3(b), assuming $T_{c0} = 500$ K, $N_{\text{eff}}V_{BCS} = 0.38$. It can be seen that N_{eff} is broader than the theoretical N , with sharper fall-off. This would be expected from a two-phase model: the superconducting phase would have an approximately constant T_c , but decreasing Meissner fraction as x is varied away from x_0 . The low-temperature Meissner fraction may, however, be nearly independent of x (as seen in the data of reference [48]), because proximity-effect coupling can drive the normal phase superconducting. On the other hand, when the superconducting fraction is small, T_c can be depressed by proximity to a normal metal or a phase with strong spin-density fluctuations.

4.5. Isotope effect

Ordinarily, it is assumed that an electronic pairing mechanism implies the absence of an isotope effect. However the present model relies on an incipient density wave, and a CDW will be accompanied by a periodic lattice distortion. Hence, there may be some isotope effect associated with this electronic mechanism as well. Unfortunately, the situation is quite complicated, and no detailed calculations can as yet be made. Nevertheless, it seems very likely that this mechanism can produce a small or even negative contribution to the isotope effect. For instance, a lighter isotope, by enhancing the phonon frequencies, would increase the CDW transition temperature. But, as discussed above, raising the CDW transition can actually decrease T_c .

4.6. Comparison with other theories

The present model is very similar to that of Varma *et al* [7], in that both assume Cu–O charge transfer excitons in the CuO_2 planes to be responsible for superconductivity. However, the distinction is significant: in the present model, the ‘excitons’ are really a CDW forming within a single band (the antibonding Cu–O band), whereas the excitons of reference [7] are true interband excitons, between the antibonding and non-bonding bands. In the latter case, the exciton gap is greater than or equal to half the bandwidth, so retardation effects are negligible, and the calculation of paper II does not yield a high T_c .

It may be possible to identify these interband transitions in optical absorption studies. In a simple picture, the interband absorption should have onsets at $E_B/2$ (antibonding \rightarrow non-bonding) and E_B (antibonding \rightarrow bonding). The observed [62] absorption peaks at 1.3 and 2.7 eV are in good agreement with the band-structure estimates of 2–3 meV. Some care must be taken, however, in accepting this assignment. There are other oxygen orbitals which can couple to the Cu, and the estimates of Stechel and Jennison [16] place them within 1 eV of the Fermi level. The model of reference [38] suggests that the strong

correlation effects greatly modify the optical properties. To get a Mott transition near half-filling requires the bare Cu–O separation to be ~ 5 eV (assuming $t_{\text{CuO}} = 1.2$ eV). Hence, even though interband transitions should be observed near both the bare and the renormalised energy gaps [41], only the renormalised bands occur within 2 eV of the Fermi level. Using the parameters of figure 8, these renormalised interband transitions have an onset near 1.1 eV, in good agreement with experiment (see paper II).

5. Conclusions

The conclusions of this paper may be conveniently summarised in terms of normal state (N) and superconducting (S) properties.

N1. Band-structure calculations are in good agreement with positron annihilation studies of the Fermi surface, but *are totally at variance with transport measurements*. In LSCO, the calculated ($\approx 1+x$) and experimental ($\approx x$) hole densities differ by a factor greater than six. This difference is usually ascribed to ‘correlation effects’, often thought of in terms of the Mott transition. However it is hard to understand how the Mott transition can be important when the hole density differs from half-filled by nearly 20%.

If, however, the Fermi surface shows considerable curvature (as predicted by band-structure calculations), then the Fermi surface will intersect the Brillouin zone boundary (van Hove singularity) at a hole concentration very different from half-filling. At this point, there should be a singularity similar to the Mott transition, but weaker, so that some holes are not involved in the transition. This transition has been identified as a (C)DW formation. Since the bands are nearly 2D, long-range order is possible only through residual 3D correlations. Since these are weak, only short-range DW order is observed.

N2. When $x \approx 0$, the physics is totally different. Here, on-site Coulomb repulsion is strong enough to produce an ordinary Mott transition (SDW) in La_2CuO_4 . Correlation effects renormalise the bands, greatly reducing the bandwidth and shifting the van Hove singularity towards half-filling [38], leading to an insulating ground state. Since the ground states are total different at $x = 0$ and $x = x_0$, there must be a first-order transition between the two, with a two-phase coexistence region.

S1. It has long been recognised that phonon-mediated pairing is inadequate to produce high- T_c superconductivity. Excitations across the (short-range) (DW) gap would appear to be an ideal candidate to produce an excitonic pairing, since they are the lowest-energy electronic excitations in the system and are strongly coupled to the low-DOS carriers (cf the large normal-state resistivity). It must be stressed that this particular mechanism does not follow automatically from the two-carrier model, but seems to offer the most plausible origin for a new attractive pairing.

6. Interpretation of the DW transition

The two-band picture of figure 3(c) might suggest a naive interpretation as a narrow, quasi-localised Cu d band overlapping a broad O p band. That this is not the case can be seen from the partial DOS calculated in figure 3(b). While the band remains mostly Cu-like, the additional O-like holes are actually added predominantly near the DOS peak. The CDW instability can therefore be interpreted in terms of a valence fluctuation. More precisely, it might be described as the formation of a covalent bond between the Cu and the O. Such an interpretation of CDW formation has been discussed previously [35, 63].

Acknowledgments

I wish to thank N Jaggi, J Zaanen, S Mazumdar and B C Giessen for very interesting conversations.

Appendix. Energy bands of equation (2)

Equation (2) is used to describe the square CuO_2 lattice. The Cu $d_{x^2-y^2}$ orbital is assumed to be coupled by t_{CuO} with a single p orbital on each near-neighbour O atom (see reference [16] for a discussion of other O orbitals). Assuming Bloch form for the wave functions, the hole bands are given by the roots of the 3×3 determinant:

$$\begin{pmatrix} \Delta E - E & y_x & y_y \\ y_x & -E & y_0 \\ y_y & y_0 & -E \end{pmatrix} = 0 \quad (\text{A.1})$$

where $y_i = 2t_{\text{CuO}} \sin(k_i a/2)$, $i = x, y$; $y_0 = 4t_{\text{OO}} \sin(k_x a/2) \sin(k_y a/2)$. If $t_{\text{OO}} = 0$, the solution simplifies. The antisymmetric p-hole combination is uncoupled, with $E = 0$ (non-bonding orbital). The bonding ($-$) and antibonding ($+$) orbitals satisfy

$$E_{\pm} = (\Delta E/2) \pm \sqrt{(\Delta E/2)^2 + y_x^2 + y_y^2}. \quad (\text{A.2})$$

If $\Delta E \gg t_{\text{CuO}}$, the antibonding band becomes

$$E_+ = \Delta E + (y_x^2 + y_y^2)/\Delta E = \Delta E + (4t_{\text{CuO}}^2/\Delta E)(2 - \cos(k_x a) - \cos(k_y a)). \quad (\text{A.3})$$

In the opposite limit $\Delta E = 0$, E_{\pm} becomes

$$E_{\pm} \equiv y_{\pm} = \pm \sqrt{y_x^2 + y_y^2} = \pm t_{\text{CuO}} \sqrt{2(2 - \cos(k_x a) - \cos(k_y a))}. \quad (\text{A.4})$$

When $t_{\text{OO}} \neq 0$, the calculations are more involved. For $\Delta E \gg t_{\text{CuO}}, t_{\text{OO}}$, perturbation theory gives for the antibonding band:

$$E_+ = \Delta E + (y_x^2 + y_y^2)/\Delta E + 2y_x y_y y_0 / \Delta E^2 \\ = \Delta E' - t_0 [(\cos(k_x a) + \cos(k_y a))(2 + \hat{t}) + \hat{t} \cos(k_x a) \cos(k_y a)] \quad (\text{A.5})$$

when $\Delta E' = \Delta E + t_0(4 + \hat{t})$ and t_0, \hat{t} are defined in equation (3). Hence, the antibonding band has the form of equation (1). In the more realistic case, with ΔE small, the solution does not have quite so simple a form. However, the resulting Fermi surfaces are similar. In the limit $\Delta E = 0$, the determinant equation can be rewritten as an equation of the constant-energy surface $k_x(k_y, E)$:

$$\cos(k_x a) = 1 - e(2e^2 - 1 + \cos(k_y a))/[e + \beta(1 - \cos(k_y a))] \quad (\text{A.6})$$

where $e = E/2t_{\text{CuO}}$, $\beta = f(1 + ef/2)$ and $f = 2t_{\text{OO}}/t_{\text{CuO}}$. The antibonding-band energy level corresponding to the van Hove singularity is just $e = 1$. In this case, if $\beta = 0$, the Fermi surface is square, as in figure 1(a), $\cos(k_x a) + \cos(k_y a) = 0$. For $t_{\text{OO}} > 0$, the Fermi surface has a similar curvature to figure 1(b). In fact, the Fermi surfaces are identical if $\beta = \hat{t}/(1 - \hat{t})$. Thus, $\hat{t} = -0.34$ is equivalent to $\beta = -0.25$, or $f = -0.3$.

References

- [1] Bednorz J G and Mueller K A 1986 *Z. Phys. B* **64** 189
- [2] Wu M K, Ashburn J R, Torng C J, Hor P H, Meng R L, Gao L, Huang Z J, Wang V Q and Chu C W 1987 *Phys. Rev. Lett.* **58** 908

- [3] Batlogg B, Kourouklis G, Weber W, Cava R J, Jayaraman A, White A E, Shon K T, Rupp L W and Rietman E A 1987 *Phys. Rev. Lett.* **59** 912
 Falten T A *et al* 1987 *Phys. Rev. Lett.* **59** 915
 Leary K J, zur Loye H-C, Keller S W, Falten T A, Ham W K, Michaels J N and Stacy A M 1987 *Phys. Rev. Lett.* **59** 1236
- [4] Bozovic I, Kirillov D, Kapitulnik A, Char K, Hahn M R, Beasley M R, Geballe T N, Kim Y H and Heeger A J 1987 *Phys. Rev. Lett.* **59** 2219
 Tajima S, Uchida S, Ishii H, Tagaki H and Tanaka S unpublished
- [5] See e.g. Capizzi M *et al* 1988 *Bull. APS* **33** 416
 Herr S L *et al* 1988 *Bull. APS* **33** 416
 Lu F *et al* 1988 *Bull. APS* **33** 416
 Weber W 1988 *Bull. APS* **33** 459
- [6] Little W A, Collman J P and McDevitt J T unpublished
- [7] Varma C M, Schmitt-Rink S and Abrahams E 1987 *Solid State Commun.* **62** 681
- [8] Mattheiss L 1987 *Phys. Rev. Lett.* **58** 1028
- [9] Xu J H, Watson-Yang T J, Yu J and Freeman A J 1987 *Phys. Lett.* **120A** 489
- [10] Jorgensen J D, Schüttler H B, Hinks D G, Capone II D W, Zhang K, Brodsky M B and Scalapino D J 1987 *Phys. Rev. Lett.* **58** 1024
 Labbe J and Bok J 1987 *Europhys. Lett.* **3** 1225
 Freidel J 1987 *J. Physique* **48** 1787
- [11] Solyom J 1979 *Adv. Phys.* **28** 201
- [12] Markiewicz R S 1989 *J. Phys.: Condens. Matter* **1** 8931–44
- [13] Markiewicz R S 1988 *High Temperature Superconductors* ed. M B Brodsky, R C Dynes, K Kitazawa and H L Tuller (Pittsburgh: MRS) p 411
- [14] Markiewicz R S 1988 *Physica C* **153–155** 1181
- [15] Markiewicz R S 1987 *Mod. Phys. Lett. B* **1** 187
- [16] Stechel E B and Jennison D R 1988 *Phys. Rev. B* **38** 4632, 8873
- [17] Yu J, Massida S and Freeman A J unpublished
- [18] Whangbo M H, Evain M, Bano M A and Williams J M 1987 *Inorg. Chem* **26** 1829, 1831, 1832
- [19] Hoffman L, Manuel A A, Peter M, Walker E and Damento M A 1988 *Physica C* **153–155** 129
 Peter M, Hoffman L and Manuel A A 1988 *Physica C* **153–155** 1724
- [20] Smedskjaer L C, Liu J Z, Benedek R, Legnini D G, Lam D J, Stahulak M D, Claus H and Bansil A 1988 *Physica C* **156** 269
- [21] Markiewicz R S 1988 *Phys. Rev. B* **38** 5010
- [22] Hybertsen M S and Mattheiss L F 1988 *Phys. Rev. Lett.* **60** 1661
- [23] Krakauer H and Pickett W E 1988 *Phys. Rev. Lett.* **60** 1665
- [24] Zaanen J, Jepsen O, Gunnarsson O, Paxton A T, Andersen O K and Svane A 1988 *Physica C* **153–155** 1636
- [25] Lee P A and Read N 1987 *Phys. Rev. Lett.* **58** 2691
- [26] Ong N P, Wang Z Z, Clayhold J, Tarascon J M, Greene L H and McKinnon W R 1987 *Phys. Rev. B* **35** 8807
- [27] Shen Z X *et al* 1987 *Phys. Rev. B* **36** 8414
- [28] Bilbro G and McMillan W L 1976 *Phys. Rev. B* **14** 1887
- [29] Gabovich A M and Shpigel A S 1984 *J. Phys. F: Met. Phys.* **14** 3031
- [30] Gabovich A M, Moiseev D P and Shpigel A S 1982 *J. Phys. C: Solid State Phys.* **15** L569
- [31] Choy T C and He H X 1987 *Phys. Rev. B* **36** 8807
- [32] Anderson P W and Abrahams E 1987 *Nature* **372** 363 and references therein
 Pouget J P, Nogera C and Moret R 1988 *J. Physique* **49** 875
- [33] Little W A 1964 *Phys. Rev.* **134** A1416
- [34] Allender D, Bray J and Bardeen J 1973 *Phys. Rev. B* **7** 1020
- [35] McMillan W L 1977 *Phys. Rev. B* **16** 643
- [36] Nagaev E L 1983 *Physics of Magnetic Semiconductors* (Moscow: MIR)
- [37] Markiewicz R S unpublished
- [38] Markiewicz R S 1989 *J. Phys.: Condens. Matter* at press
- [39] Hume-Rothery W and Raynor G V 1962 *Structures of Metals and Alloys* 4th edn (London: Institute of Metals)
- [40] Heine V 1969 *Electrons in Metals* ed. J M Ziman (Cambridge: Cambridge University Press) p 1
- [41] Kotliar G, Lee P A and Read N 1988 *Physica C* **153–155** 538
- [42] Hinks D G, Dabrowski B, Zhang K, Segre C U, Jorgensen J D, Soderholm L and Beno M A 1988 *High Temperature Superconductors* ed. M B Brodsky, R C Dynes, K Kitazawa and H L Tuller (Pittsburgh: MRS) p 9

- [43] van Dover R B, Cava R J, Batlogg B and Rietman E A 1987 *Phys. Rev. B* **35** 5337
- [44] Tarascon J M, Greene L H, McKinnon W R, Hull G W and Geballe T H 1987 *Science* **235** 1373
- [45] Venturini E L private communication
- [46] Uher C and Kaiser A B 1988 *Phys. Rev. B* **37** 127
- [47] Grant P M, Parkin S S P, Lee V Y, Engler E M, Ramirez M L, Vazquez J E, Lim G, Jacowitz R D and Green R L 1987 *Phys. Rev. Lett.* **58** 2482
- [48] Torrance J B, Tokura Y, Nazzari A I, Bezinga A, Huang T C and Parkin S S P 1988 *Phys. Rev. Lett.* **61** 1127
- [49] Markiewicz R S, Chen K and Jaggi N 1987 *Phys. Rev. B* **37** 9336
- [50] Schrieffer J R, Wen X-G and Zhang S-C 1988 *Phys. Rev. Lett.* **60** 944
- [51] Hirsch J E, Tang S, Loh Jr E and Scalapino D J 1988 *Phys. Rev. Lett.* **60** 1668
- [52] Shirane G, Endoh Y, Birgeneau R J, Kastner M A, Hidaka Y, Oda M, Suzuki M and Murakami T 1987 *Phys. Rev. Lett.* **59** 1613
- [53] Lee P A, Rice T M and Klemm R A 1977 *Phys. Rev. B* **15** 2984
- [54] Bhattacharya S, Higgins M J, Johnston D C, Jacobson A J, Stokes J P, Goshorn D P and Lewandowski J T 1988 *Phys. Rev. Lett.* **60** 1181
- [55] See, e.g. Boolchand P, Enzweiler R N, Zitkovsky I, Wells J, Bresser W, McDaniel D, Meng R L, Hor P H, Chu C W and Huang C Y 1988 *Phys. Rev. B* **37** 3766
Golovashkin A I, Danilov V A, Ivanenko O M, Mitsen K V and Perepechko I I 1987 *Pis'ma Zh. Eksp. Teor. Fiz.* **46** 273 (Engl. Transl. 1987 *JETP Lett.* **46** 343)
- [56] Mazumdar S 1989 *Chemistry of Oxide Superconductors* to be published
- [57] Sarma D D and Rao C N R 1987 *J. Phys. C: Solid State Phys.* **20** L659
Dauth B, Kachel T, Sen P, Fischer K and Campagna M 1987 *Z. Phys.* **B 68** 407
Kachel T, Sen P, Dauth B and Campagna M 1988 *Z. Phys.* **B 70** 137
- [58] Tarascon J M, McKinnon W R, Greene L H, Hull G W, Bagley B G, Vogel E M and Le Page Y 1987 *Proc. MRS* ed. D U Gubser and M Schluter at press
- [59] Siegrist T, Zahurak S M, Murphy D W and Roth R S 1988 *Nature* **334** 231
- [60] Tarascon J M *et al* unpublished
Greene L H 1988 *Bull. APS* **33** 212
- [61] Tesanovich Z 1987 *Phys. Rev. B* **36** 2364. A measure of the ratio $\Delta E_{3D}/E_B$ is given by the conductivity anisotropy, which is ≥ 100 in YBCO single crystals and considerably higher in the Tl and Bi compounds. In fact, this anisotropy is increasing as T decreases, and P W Anderson and Z Zhou 1988 (*Phys. Rev. Lett.* **60** 132) have suggested that the ratio diverges ($\Delta E_{3D} \rightarrow 0$) as $T \rightarrow 0$.
- [62] Herr S L, Kamaras K, Porter C D, Doss M G, Tanner D B, Bonn D A, Greedan J E, Stager C V and Timusk T 1987 *Phys. Rev. B* **36** 733
Etemad S, Aspnes D E, Kelly M K, Thompson R, Tarascon J M and Hull G W 1988 *Phys. Rev. B* **37** 3396
- [63] Cohen M L and Anderson P W 1972 *Superconductivity in d- and f-Band Metals* ed. D H Douglass (New York: American Institute of Physics) p 17